

What is the Role of Shear Force in Granular Crystallization?

3 † Fei Wang, † Yi Cai, and † Yrjö Jun Huang (黃 駿)*

4 †Department of Aeronautics and Astronautics, Fudan University, Shanghai, China

5 Granular compaction is the process in which an excitation is applied to the granular materials and the volume fraction, or density, increases. A recently experiment reported that twisting a large number of cubic particles in a cylinder container leads to an ordered packing. In this article, this phenomenon is repeated by using discrete element method (DEM) simulation. Furthermore, different gravitations are used and it is found that a suitable gravitation is also a very important parameter. In addition, a twisting chamfering cylinder container and a shaking cubic container are simulated. It is found the rectangle angles between the side walls and the bottom plays a key role in such kind of ordering process.

PACS numbers: 45.95.+x, 45.70.Mg, 02.60.Cb

I. INTRODUCTION

7 Granular material is a conglomeration of huge number 48 of discrete macroscopic particles. The behaviors of gran- 49 uar material is neither similar to that of liquid, gas or 50 solid, it becomes one of the most mysterious problems in 51 modern sciences [3]. The granular compaction is one of 52 those unique behaviours. It is a process of increasing the 53 volume fraction of granular material subjected to shak- 54 ing, tapping, twisting, and some other kinds of external 55 excitation. Various experimental studies show that the 56 dynamics of granular compaction is a complex problem 57 [1, 4–9]. On the other hand, some models are raised to 58 identify the physics underlying granular compaction [10– 59 13]. Among these experiments, Reis *et al.* [7] experimen- 60 tally investigated the structural changes from disordered 61 state to ordered state of a 2-D granular system. At the 62 same time, Daniels & Beheinger [8] investigated a 3-D 63 system composed of spheres. Both of these two groups 64 made an analogy between their respective granular sys- 65 tem and molecule crystallization process. This structural 66 change process is called granular crystallization. Recent- 67 ly, Asencio *et al.* [9] applied alternating rotations, or 68 “twist” to a cylindrical container with cubic particles. It 69 is a highly efficient way to achieve ordered packing of 70 morphologies of concentric rings. They suggested that 71 “*the ordering process is a competition between the shear imposed by the cylindrical container and the load carried out by the dice column*”.

Numerical simulation is a third way next to experi- 72 ments and theoretical models in the study of natural, 73 artificial, and abstract systems and processes. Discrete 74 element method (DEM) is a family of numerical methods 75 for computing the motion of a huge number of small par- 76 ticles. In this article, DEM simulations are carried out to 77 analysis this ordering process of cubes in a cylinder. The 78 simulations show that the shear force acts as a hindrance 79 in crystallization. In additional, a perpendicular sidewall 80 to the bottom and a great enough gravitation are also 81 important in this process.

To show our opinion, the structure of this article is or-

ganized as follows. A brief introduction of the numerical method is given in of section II. In section III, the simulational results are presented. Based on these simulations, the conclusions are drawn in the last section.

II. DEM MODEL

The DEM is based on the Lagrangian approach to simulate the motion of each particle in a granular system. It was firstly created by Cundall in 1970s for rock mechanics [14]. Disk shaped 2-D particles or spherical particles are used in the early stage of the development of DEM. The uniform and regular profiles requires a simple algorithm, which leads to a highly efficient computing performance. However, asymmetrical, namely complex shaped, particles are widespread in the granular system in industries. Several methods are developed to describe the profile of a complex particle, such as sphere intersection method [15], cylinder-sphere method [16, 17], interaction laws for ambiguous contact convex polygonal particles [18], superellipsoid method [19, 20] and so on.

In this article, the simulations were carried out by a DEM software named Åpen diskret element metoden (ÅDEM, Open Discrete Element Method in Norwegian). In this software, glued particle method (GPM), also named multi-sphere particle method [21, 22], is employed for a complex particle. Two Cubic particles formed by this method as shown in Fig.1(a). The central particles are named host particles and the rest 26 particles in each cube are named slave-particles. For each cube, the slave-particles only indicate the geometric profile of the cubic particle, while the rest information about the cube is carried by the central particle, such as mass, material properties, spatial attitude, location of mass center and so on. In other words, the binary cube-cube collision in Fig.1(a) becomes a binary slave-slave particles collision.

It is well known that the coefficient of restitution (CoR), e , is related to particle size, material, initial velocity and so on, complicatedly [23–25]. To simple the question, a constant CoR ($e = 0.1$) is used in all of our

*Electronic address: jun_huang@fudan.edu.cn

simulations. Thus, the spherical-spherical particle contact process is modelled as a spring-dashpot system. The normal force is a sum of an elastic term and a viscous term at the contact point, that

$$F_n = F_n^e + F_n^d = K_n \delta_n^\zeta + \eta_n \delta_n^\xi \dot{\delta}_n \quad (1)$$

The details of all coefficients are introduced Ref.[30]. On the other hand, the magnitude of the tangential force, $|\mathbf{F}_{t,i}|$, is obtained from Coulomb's friction law, that, $|\mathbf{F}_{t,i}| = \mu |\mathbf{F}_{n,i}|$. The Standard Euler Method was employed for the time integration algorithm for velocity and position of each particle, that $\mathbf{u}' = \mathbf{u} + \sum \mathbf{F} dt / m$ and $\boldsymbol{\Omega}'_{n,t} = \boldsymbol{\Omega}_{n,t} + \sum (\mathbf{F} \times \mathbf{L}) dt / I$, where the primes mean the state after the time step dt , the corresponding symbols without prime are the state before the time step. I is the momentum of inertia. For cube, $I = ms^2/6$, where s is the length of the edge. \mathbf{L} is the vector from the centre of the host particle to the contact point.

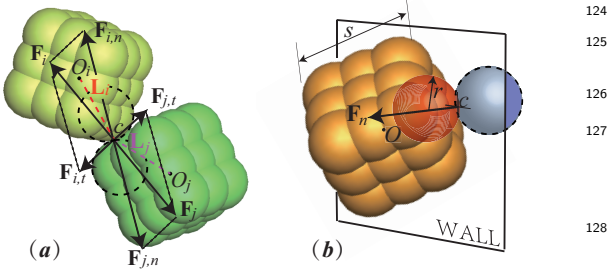


FIG. 1: Collision Model: (a) Cube-Cube collision. Each cubic particle is composed of 27 small slave spherical particles. The collision happens between the two circled particle. (b) Cube-wall collision. The red particle is one of a slave spherical contacting with the wall and the blue one is a ghost particle to replace the wall.

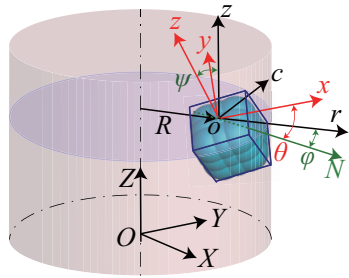


FIG. 2: Three coordinate systems and Euler angles: X, Y and Z are the globe Cartesian coordinates; r, c and z is the cylindrical coordinates; and x, y and z are the local Cartesian coordinates. θ, ϕ and ψ are Euler angles.

An ordered system means that there are a series of concentric rings stacked in horizontal layers in Asencio *et al.*'s experiment. In order to quantify the centripetal level, three coordinate systems are used. The first is the globe Cartesian coordinate system, X, Y and Z . Because it is easy to calculate the relative velocity and relative position between any two particles, most of the program is run in this system. The second coordinate system is the local Cartesian coordinates, x, y and z . The origin of this coordinate is located in the center of one side of a cube, o , and the coordinates are parallel to the edges. The last coordinate system is the cylindrical coordinates, r, c and z . Three Euler angles, θ, ϕ and ψ are used for the conversion between the cylindrical and the local Cartesian coordinates. Due to the symmetry of a cube, the range of each angel is limited between 0 and $\pi/2$. A normalized value of the Euler angles, α , is used to quantify the centripetal level, that $\alpha = \frac{2}{3\pi}(\theta + \phi + \psi)$. In other words, $\alpha = 0$ means the orientational of the cubes is perfect centripetal. While $\alpha = 1$ means that the cubes is maximum offset from the perfect state. For the whole system, an averaged centripetal level $\bar{\alpha}$ is introduced, that $\bar{\alpha} = \frac{\sum_{i=1}^N \alpha}{N}$. Here N is the number of cubes in the system.

III. SIMULATIONS AND COMPARISONS

Totally seven simulations are presented in this article. Generally speaking, simulations can be divided into two groups. The simulations in the first group (Cases 1-4) are the natural acculturational process only under gravity, while the others (Cases 5-7) are the crystallization processes with external excitation. In detail, the effect due to the containers with geometrical profiles are compared between Case 1 and Case 2. While, the effect from the different gravitations are compared between Cases 1, 3 and 4. This comparison with different surface friction is carried out among Cases 5-7.

A. Planer bottom vs. Concave bottom

Asencio *et al.* used twenty thousands cubes in their experiment [9]. Due to the limited computing power, a mini sized cylindrical container with diameter $D = 10\text{ cm}$ is used in our simulation. Totally 1080 uniform cubes of edge $s = 1\text{ cm}$ are put in the container. To repeat Asencio *et al.*'s experiment numerically, the cubes should be densely, steadily and randomly packed in the container at the very beginning. Hence the first simulation employing anneal method was carried out firstly to achieve this initial state. All these cubes were created in the cylindrical container loosely. The position, space spatial attitude and velocities of each cube are random. Furthermore, there is no overlap between any two cubes. A downward

For particle-wall collision, a mirror symmetrical ghost particle is created to take place one particle in the aforementioned binary collision model. More details of the collision models in ADEM was introduced in ref [30].

gravitation is added to all cubes. the cubes accumulate₁₆₃ on the bottom of the container due to the gravitation.₁₆₄ To speed the accumulating process, a low CoR, $e = 0.2$ ₁₆₅ and a great gravitation, $g_1 = 29.4m/s^2$ are used. The₁₆₆ final state from this simulation, which means the kinetic₁₆₇ energy approaches to zero, will be used as the initial₁₆₈ states in Cases 5-7.

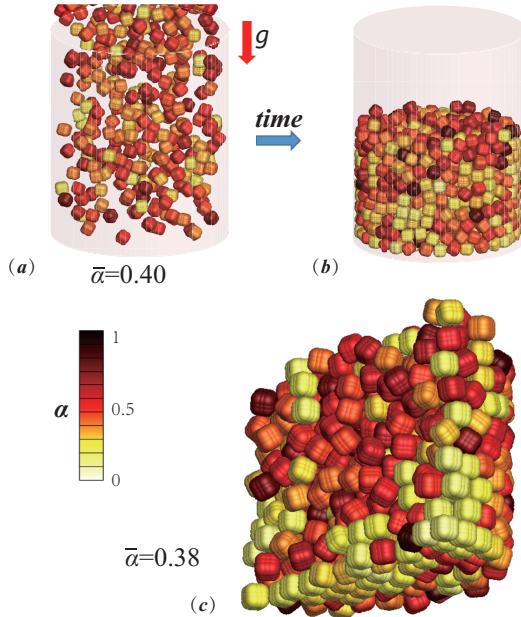


FIG. 3: Simulational results of Case 1: (a) $t = 0$; (b) final state of $t = 3s$ and (c) a cut-away view of the final state. The color shows the quantity of the centripetal level, α .

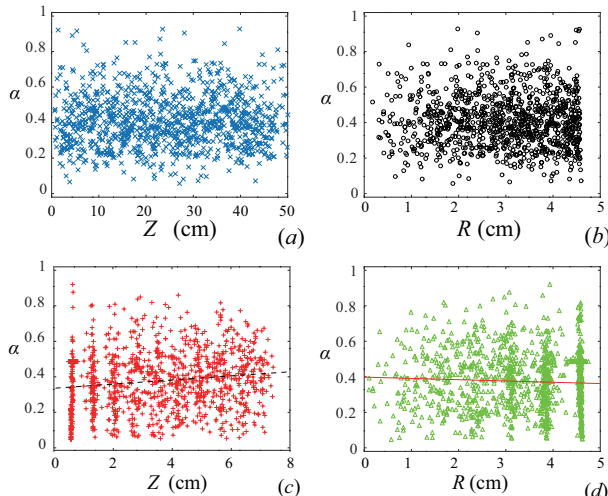


FIG. 4: The relations between the position and α . (a) α against height in the initial state; (b) α against radius in the initial state; (c) α against height in the final state and (d) α against radius in the final state.

The simulational results are plotted in Figs.3 & 4. From Fig.3, it can be seen that the color of those cubes₁₈₄

near the sidewall and the bottom is much more close to white than those in the center or upper surface. In detail, the distributions of the dimensionless disorder index α and linear data fitting lines using least square method (LSM) are plotted in Fig.4. It can be seen that the values of α are random about the horizontal axis in both Figs.4 (a) and (b). While the horizontal layers in Fig.4(c) and the centripetal layer in Fig.4(d) are obvious, especially in the upper left corner of Fig.4 (c) and upper right corner of Fig.4(d).

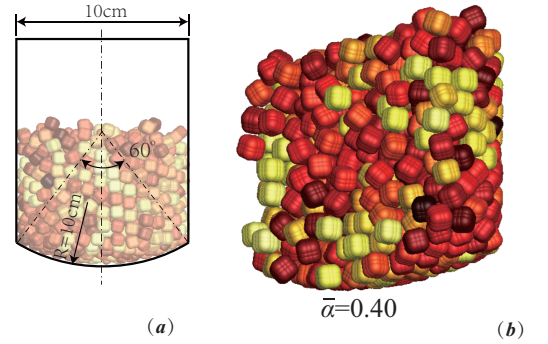


FIG. 5: Simulation results of Case 2: (a) profile of the container with a lightly concave bottom and (b) a cut-away view of the final state. The color shows the quantity of the centripetal level, α .

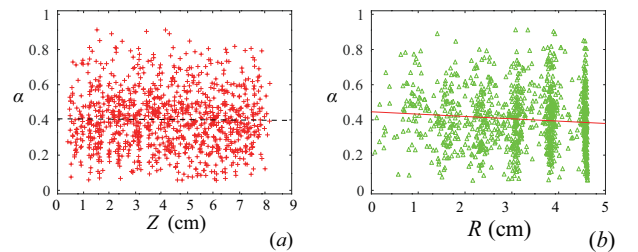


FIG. 6: The relations between the position and α in Fig.5(b). (a) α against height and (b) α against radius.

In Case 1, the cubes are well-bedded near the side wall and the bottom. This phenomena hints there exists a possible boundary effect. To prove this inspection, Case 2 was carried out. A lightly convex bottom is used in this simulation. The geometrical profile is shown in Fig.5(a). The other initial conditions are exactly the same as those in Case 1, such as the number of particles, gravitation, diameter of the container and so on. Figs.5 & 6 present the results. It is obvious that the well-bedded structure near the boundaries are destroyed, especially for those near the bottom. The α fitting line is almost a constant along the vertical direction (Fig.6(a)).

B. Effect from the gravitation

In Refs. [7–9], a dimensionless acceleration Γ is introduced, which is the ratio between the external excitation and gravitation. This dimensionless acceleration plays an important role in the crystallization process. Thought the external excitation does not exist for accumulation problems, the role of gravitation is also observed in our simulations. Keep the same parameters of Case 1 and different gravitations are used, that $g_3 = 3g_1 = 29.4m/s^2$ in Case 3 and $g_4 = 10g_1 = 98.0m/s^2$ in Case 4 respectively. The accumulated cubes under different gravitations are presented in Figs.7 and 8. For lower gravitation, it takes a longer time to achieve the accumulated state, and therefore Figs.7(a) & 8(a) presents the state of Case 3 at $t = 1.0s$, while the other figures present the states at $t = 0.5s$.

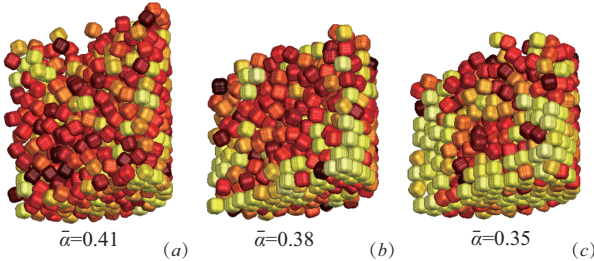


FIG. 7: Accumulated states under different gravitation. (a) Case 3: $g_1 = 9.81m/s^2$ at $t = 1.0s$; (b) Case 1: $g_2 = 3g_1 = 29.4m/s^2$ at $t = 0.5s$ and (c) Case 4: $g_3 = 10g_1 = 98.1m/s^2$ at $t = 0.5s$.

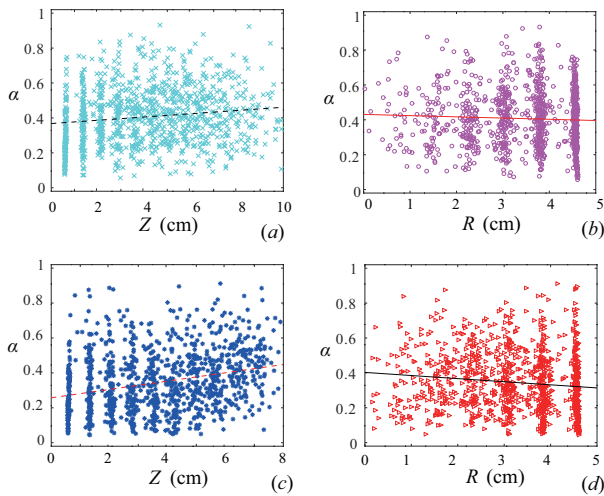


FIG. 8: The relations between the position and α for the states in Fig.7. (a) Case 3 and (b) Case 4. The straight lines are data fitting using LSM.

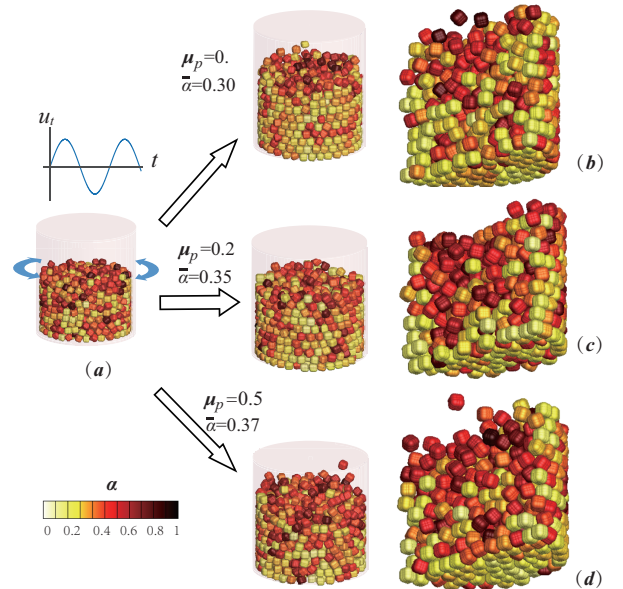


FIG. 9: Simulation results with different surface friction μ_p under the same external excitations after three seconds: (a) the initial state; (b) Case 5; (c) Case 6 and (d) Case 7. The color shows the quantity of the centripetal level, α .

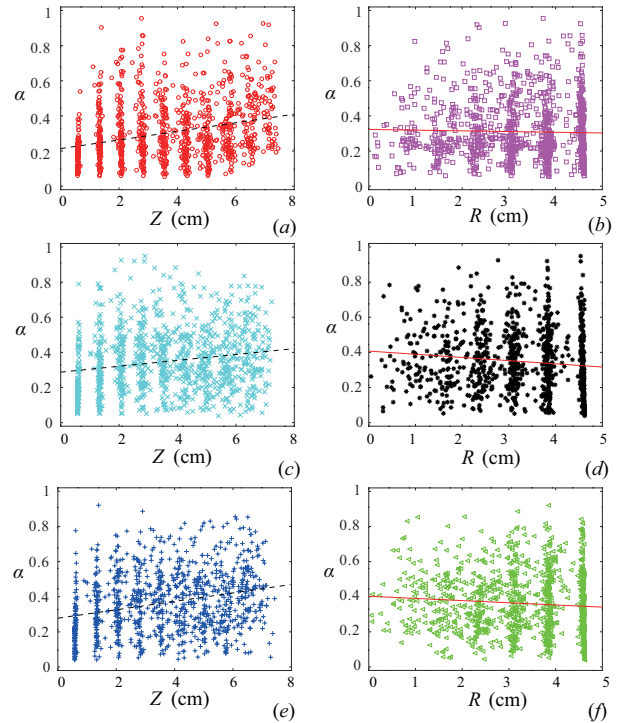


FIG. 10: The relations between the position and α in Fig.9(b-d). (a) α against height for Case 5; (b) α against radius for Case 5; (c) α against height for Case 6; (d) α against radius for Case 6; (e) α against height for Case 7 and (f) α against radius for Case 7.

201 C. Effect from the Surface Roughness 220

202 For Cases 5-7, all the initial positions of all cubes are 222
 203 loaded from the finial results of Case 1, which is shown 223
 204 in Fig.3(b & c). A sinusoidal velocity, u_t , is added 224
 205 to the sidewall in the tangential direction, as shown in 225
 206 Fig.9(a), that $u_t = U_{max} \sin(\omega t)$, where $U_{max} = 1m/s^{226}$
 207 and $\omega = 20s^{-1}$. Different surface friction among parti- 227
 208 cles μ_p are used, that $\mu_p=0$, 0.2 and 0.5 for each case 228
 209 respectively. The drive power is from the motion of the 229
 210 side and wall and therefore the friction coefficient be- 230
 211 tween the particles and walls are same for these Cases 231
 212 that $\mu_w = 0.2$. The finial results at $t = 4s$ are presented 232
 213 in Figs.9 & 10. The lower surface friction μ_p used, the 233
 214 more ordered packed cubes is. This shows that the shear 234
 215 force is not the driving power for crystallization. On the 235
 216 contrary, it acts as a hindrance. 236
 217

IV. CONCLUSIONS

218 Discrete element method (DEM) is used to simulate
 219 the process of ordering of cubes with a periodical ex-

-
- 239 [1] P. Richard, M. Nicodemi, R. Delannay, P. Ribiere, and 270
 240 D. Bideau, *Nature Materials* **4**, 121 (2005). 271
- 241 [2] M. Paulick, M. Morgeneyer, and A. Kwade, *Granular* 272
 242 *Matter* **17**, 83 (2015). 273
- 243 [3] H. M. Jaeger, S. R. Nagel, and R. P. Behringer, *Physics* 274
 244 *Today* **49**, 32 (1996). 275
- 245 [4] J. B. Knight, C. G. Fandrich, C. N. Lau, H. M. Jaeger, 276
 246 and S. R. Nagel, *Physical Review E* **51**, 3957 (1995). 277
- 247 [5] P. Philippe and D. Bideau, *Physical Review Letters* **91**, 278
 248 104302 (2003). 279
- 249 [6] C. M. Pica, M. Nicodemi, and A. Coniglio, *Physical* 280
 250 *Review E* **75**, 021303 (2007). 281
- 251 [7] P. M. Reis, R. A. Ingale, and M. D. Shattuck, *Physical* 282
 252 *Review Letters* **96**, 258001 (2006). 283
- 253 [8] K. E. Daniels and R. P. Behringer, *Physical Review Let-* 284
 254 *ters* **94**, 168001 (2005). 285
- 255 [9] K. Asencio, M. Acevedo, I. Zuriguel, and D. Maza, *Phys-* 286
 256 *ical Review Letters* **119**, 228002 (2017). 287
- 257 [10] E. Caglioti, V. Loreto, H. J. Herrmann, and M. Nicode- 288
 258 mi, *Physical Review Letters* **79**, 1575 (1997). 289
- 259 [11] M. Nicodemi, A. Coniglio, and H. J. Herrmann, *Physical* 290
 260 *Review E* **55**, 3962 (1997). 291
- 261 [12] J. J. Brey and A. Prados, *Physical Review E* **68**, 051302 292
 262 (2003). 293
- 263 [13] G. S. Boltachev, N. B. Volkov, V. V. Ivanov, and 294
 264 S. N. Paranin, *Journal of Applied Mechanics & Technical* 295
 265 *Physics* **49**, 336 (2008). 296
- 266 [14] P. A. Cundall, in *Proceedings of the Symposium of Inter-* 297
 267 *national Society for Rock Mechanics* (ISRM, 1971). 298
- 268 [15] P. A. Langston, M. A. Al-Awamleh, F. Y. Fraige, and 299
 269 B. N. Asmar, *Chemical Engineering Science* **59**, 425
 (2004).
- 270 [16] M. Allen, D. Frenkel, and J. Talbot, *Computer physics* 271
 271 *reports* **9**, 301 (1989).
- 272 [17] A. Džiugys and B. Peters, *Granular Matter* **3**, 231 (2001).
- 273 [18] D. Markauskas, R. Kačianauskas, A. Džiugys, and 274
 274 R. Navakas, *Granular Matter* **12**, 107 (2010).
- 275 [19] R. Wait, *Mathematical Modelling and Analysis* **6**, 156 276
 (2001).
- 277 [20] C. Wang, C. Wang, and J. Sheng, *International Journal* 278
 278 *for Numerical and Analytical Methods in Geomechanics* 279
 279 **23**, 815 (2015).
- 280 [21] G. Lu, J. R. Third, and C. R. Muller, *Chemical Engi- 281
 281 neering Science*.
- 282 [22] W. Zhong, A. Yu, X. Liu, Z. Tong, and H. Zhang, *Powder* 283
 283 *Technology* **302**, 108 (2016).
- 284 [23] F. G. Bridges, A. Hatzes, and D. N. C. Lin, *Nature* **309**, 285
 333 (1984).
- 286 [24] F. G. Bridges, K. D. Supulver, D. N. C. Lin, R. Knight, 287
 287 and M. Zafra, *Icarus* **123**, 422 (1996).
- 288 [25] M. Hu, Y. J. Huang, F. Wang, and M. S. Foss, *Journal* 289
 289 *of Applied Mechanics* **85**, 041006 (2018).
- 290 [26] K. L. Johnson, *Contact mechanics* (Cambridge university 291
 291 press, 1987).
- 292 [27] R. Mindlin and H. Deresiewica, *Journal of applied me- 293
 293 chanics* **20** (2013).
- 294 [28] G. Kawabara and K. Kono, *Jpn. J. Appl. Phys. 1* **26**, 295
 1230 (1987).
- 296 [29] L. Verlet, *Physical Review* **165**, 201 (1968).
- 297 [30] D. Su, Y. X. Wang, Y. J. Huang, and A. M. Zsaki, 298
 298 *Powder Technology* **313** (2017).